Live Cell Imaging of the Actin Cytoskeleton Using the Fluorescent Probe SiR-Actin and CELLAVISTA®

Schaefer W[1], Geisen R[1], Sebens S[2] & Pirsch M[1]
[1]SYNENTEC GmbH, Elmshorn, Germany
[2]Institute for Experimental Cancer Research, CAU + UKSH Kiel, Germany

ABSTRACT

Many essential cellular processes like cell migration, axonal growth, phagocytosis, cytoplasmic streaming and organelle transport would not take place without the cytoskeleton. One important part of it is the actin cytoskeleton. A relatively new tool to study actin in living cells is the non-toxic and highly specific F-actin-labelling probe SiR-actin, whose near-infrared fluorophore is switched on by binding. Here, we analyzed its suitability for high-content applications. With our automated microscope CELLAVISTA®, we could image SiR-actin-labelled F-actin over time in living cells. We observed cellular structures formed by actin like stress fibers, the actin cortex or the cytokinetic contractile ring. Moreover, we inhibited actin polymerization by cytochalasin D and observed the induced changes over time. Using our *Real Cytoplasm (1F)* application, SiR-actin intensity was analyzed in a combined staining with the DNA dyes Hoechst33342 or SPY505-DNA. In summary, SiR-actin probes in combination with our automated imagers CELLAVISTA® or NYONE® are great tools to analyze cellular processes in high-content screening.

KEYWORDS: SIR-ACTIN, LIVE IMAGING, CYTOCHALASIN D, CYTOSKELETON, DRUG SCREENING, ACTIN DYNAMICS, PHALLOIDIN,

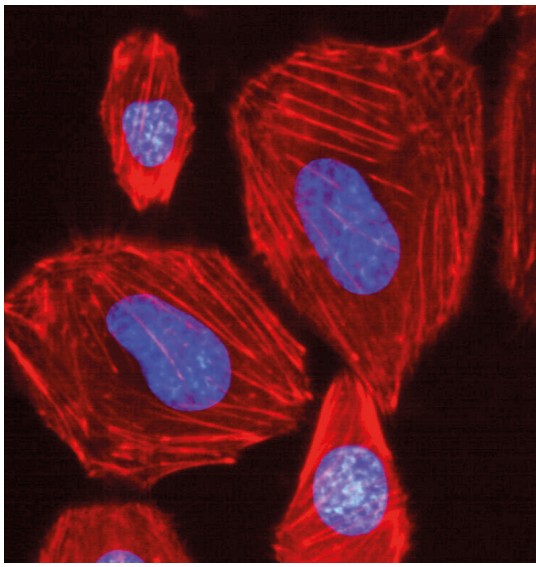

INTRODUCTION

The actin cytoskeleton contributes to important cellular functions including the basic framework of the cell shape, movement, interactions with other cells and intracellular organizations [1], [2]. For this, actin is organized in different structures like branched and crosslinked networks, parallel bundles and anti-parallel structures [3]. These structures are forming lamellipodia, filopodia, the cortex and 3D network including stress fibers. Lamellipodia and filopodia are responsible for the movement of cells. Lamellipodia move in the direction in which the filopodia point by polymerizing the actin filaments [3]. The cortex and 3D network of actin connects cells to the extracellular matrix. This is done by the binding of stress fibers to adhesion sites. Moreover, they ensure the formation and change of cell morphology [2], [3]. For example, the morphological change to the mitotic round cell shape happens through the enrichment of actin as a rigid actomyosin network (actin cortex) under the plasma membrane [4]. The round cell shape protects the mitotic process in the cell and the alignment of the spindle depends on the cell shape [4]. At the end of mitosis, actin forms the contractile ring for cytokinesis [2]. For the different functions of actin, globular actin (G-actin) needs to assemble to filamentous actin (F-actin), which can disassemble again (Fig. 1) [1]. F-actin has polar ends, named pointed and barbed end, where the polymerization and depolymerization is ATP/ADP-driven with different kinetics [5], [6]. To study changes in the actin cytoskeleton by microscopy including high-content screening, visualisation of actin is necessary. Traditional methods of visualizing F-actin like phalloidin staining usually require fixation of cells [7]. Some newer live cell imaging techniques use genetically encoded fluorescently tagged actin (e.g. CellLight®, Actin-GFP or other GFP-actin probes) or actin-binding domains instead. One widely used example are LifeAct dyes (ibidi GmbH) [7].

Here, we describe imaging of the actin cytoskeleton in living cells using the probe SiR-actin. SiR-actin is a fluorogenic and cell permeable F-actin labelling probe for living cells. SiR-actin is based on the fluorophore silicon rhodamine (SiR), a silicon-substituted xanthene dye [8], [9]. SiR is conjugated to desbromo-desmethyl-jasplakinolide, which is non-toxic and binds highly specific to F-actin [10], [11]. Binding of SiR-actin to polar F-actin activates its fluorescence [10]. As it circumvents any time-consuming cell transfection and protein overexpression systems, SiR-actin can be easily used in imaging approaches [7].

Due to its various roles, actin is an interesting target for new drugs

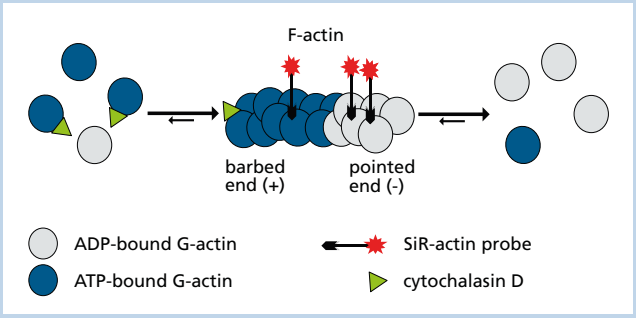

FIG. 1. ACTIN POLYMERIZATION AND DEPOLYMERISATION

The filamentous actin (F-actin, polymer) is mainly assembled at the barbed end (+) by polymerization of ATP-bound globular actin (G-actin, monomer) and disassembled at the pointed end (-). The SiR-actin probe binds between contact points of the monomers in the polymer. Cytochalasin D binds to the barbed end and prevents polymerization and also stimulates the hydrolysis of ATP bound at the G-actin (based on Milroy et al. [11]).

and thus, assays analyzing actin dynamics would be interesting for high-content screening approaches. Here, we used SiR-actin staining to observe the cellular effects of cytochalasin D. This fungal metabolite binds to the barbed end of F-actin with high affinity and stimulates ATP-hydrolysis of G-actin. By doing so, it inhibits actin polymerization and induces depolymerization (Fig. 1) [5], [12], [13]. To use our *Real Cytoplasm (1F)* application, we combined SiR-actin staining with the two DNA dyes Hoechst33342 or SPY505-DNA, which is a fluorogenic green DNA probe suitable for live cell imaging [14]. The aim of this Application Note was to demonstrate the suitability of our imagers CELLAVISTA® or NYONE® for the imaging and analysis of the cytoskeleton in a live imaging manner.

MATERIAL

- CHO-K1 cells (Chinese hamster ovary cell line)
- DMEM/F-12 (e.g. Gibco Cat. No. 21331020) supplemented with 10 % (v/v) heat inactivated FCS, 1 % (v/v) glutamine
- Trypsin 0.05 %/ EDTA 0.02 % (e.g. PAN Biotech)
- 96 well plate (e.g. Greiner Cat. No. 655891)
- Verapamil (20 mM in DMSO, e.g. Sigma Cat. No. V4629)
- Hoechst33342 (5 mg/mL, e.g. Invitrogen Cat. No. H1399)
- SiR-actin (1 mM in DMSO, Spirochrome Cat. No. SC001)
- SPY505-DNA (1000 x in DMSO, Spirochrome Cat. No. SC101)
- Cytochalasin D (from Zygosporium mansonii; 5 mg/mL in DMSO, 0.2 µm-filtered; e.g. Sigma Aldrich Cat. No. C2618)
- DMSO (e.g. Invitrogen Cat. No. D12345)

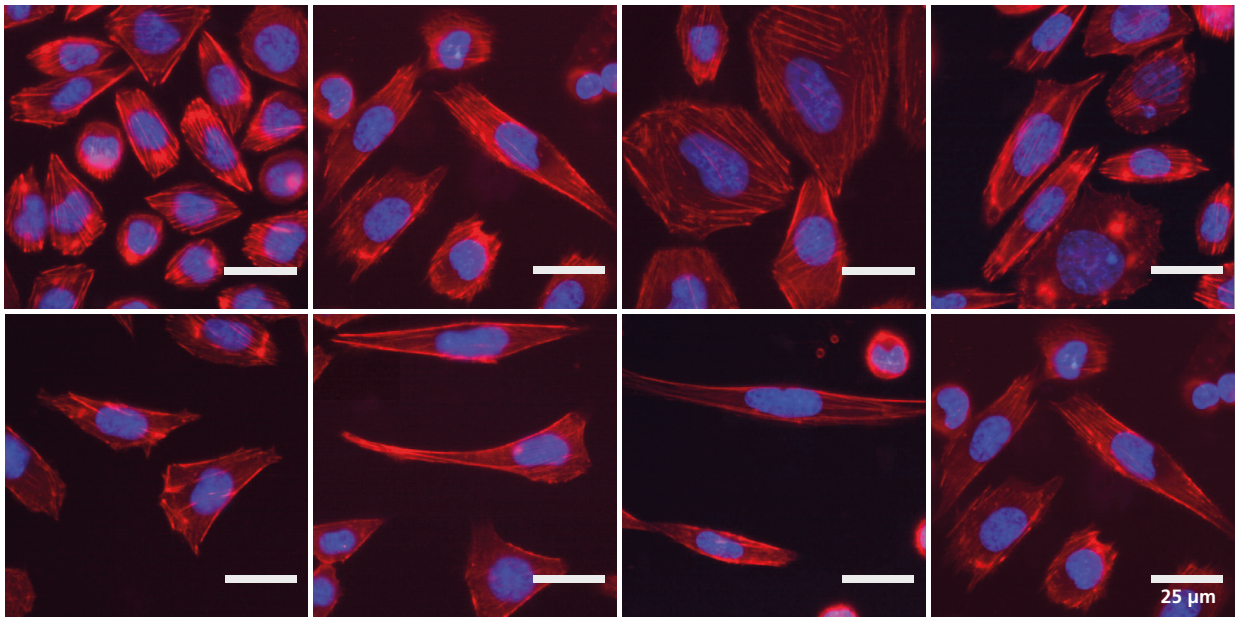

FIG. 2. SiR-ACTIN-STAINED STRESS FIBERS

We seeded 4 x 10^3 CHO-K1 cells per well in a black 96 well plate and stained the cells for one hour with SiR-actin (red) plus verapamil and Hoechst33342 (blue). Stress fibers were visible by imaging the cells with CELLAVISTA® (40x objective, scale bar: 25 µm).

METHODS

Cell Culture and Cell Counting

We routinely cultured CHO-K1 cells in DMEM/F-12 medium containing FCS (see above) using standardized cell culture conditions (37 °C, 5 % CO_2, humidified atmosphere). They were trypsinized and then counted using SYNENTEC's *Trypan Blue* application.

Labelling and Treatment of Cells

For live staining, we seeded 4 x 10^3 cell/well in a black, glass and flat bottom 96 well plate and cultivated the cells for two days. SiR-actin and SPY505-DNA stock solutions (1000x) were prepared by adding 50 µL DMSO to the vials. The old medium was removed and replaced with one of the three labelling solutions:

1. verapamil 10 µM + SiR-actin (1x)
2. verapamil 10 µM + SiR-actin (1x) + SPY505-DNA (2x)
3. verapamil 10 µM + SiR-actin (1x) + Hoechst (2 µg/mL)

Verapamil was needed to inhibit efflux pumps and acquire a uniform staining of all cells. Cells were labelled for one hour at 37 °C, after which the labelling solutions were replaced with normal medium with or without cytochalasin D.

Imaging and Image Analysis

Imaging was performed using the 40x objective of CELLAVISTA® before and after treatment with cytochalasin D for 2 h. Nine images were acquired per well. Image analysis was performed using YT®-software.

TAB. 1: IMAGING SETTINGS

Channel	Excitation LED [nm]	Emission Filter [nm]
Hoechst33342	UV (377/50)	Blue (452/45)
SPY505-DNA	Blue (475/28)	Green (530/43)
SiR-actin	Red (632/22)	Far Red (685/40)

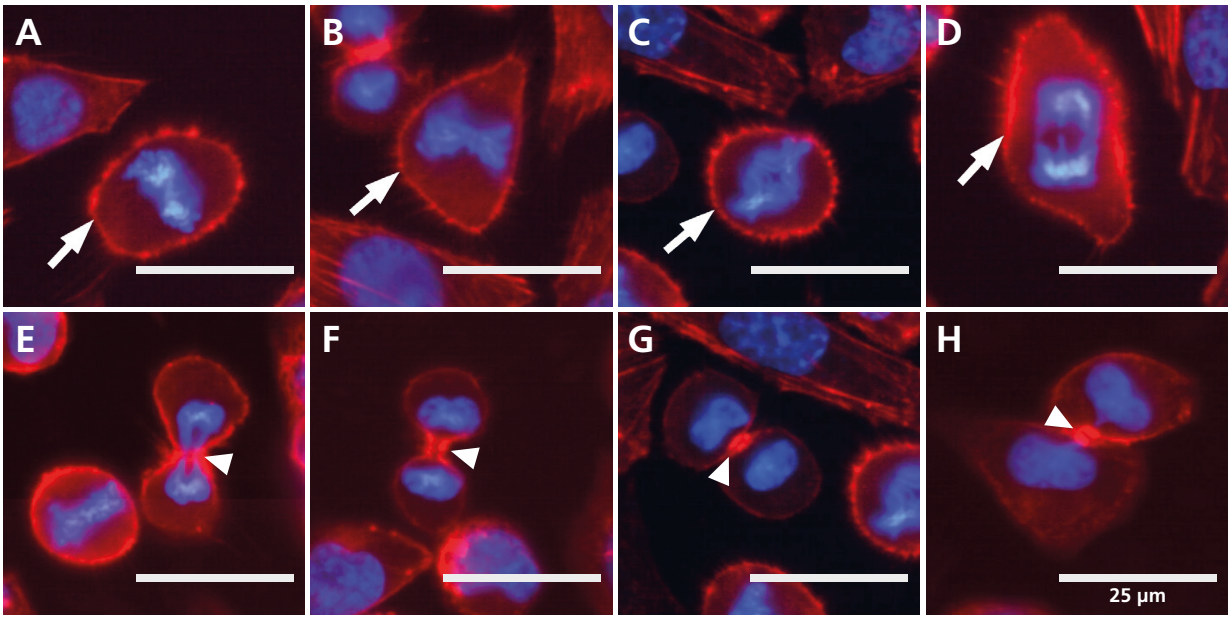

FIG. 3. SiR-ACTIN-STAINED CELLS DURING MITOSIS

We seeded 4 x 10^3 CHO-K1 cells per well in a black 96 well plate and stained the cells for one hour with SiR-actin (red) plus verapamil and Hoechst33342 (blue). Various cells in different mitotic stages were present. At early phases, Hoechst-stained DNA started to condense into chromosomes, which aligned in the equatorial metaphase plate (A,B). Subsequently, sister chromatids were separated (C,D) and lastly (E-F), the cell divided into two daughter cells. In early phases (A-D), a bright actin signal was observed at the cell periphery (white arrow), indicating the presence of the actomyosin cortex. During cytokinesis, a strong actin staining was visible in the cleavage furrow, most likely resembling the contractile ring (white arrow head, 40x objective, scale bar: 25 µm).

RESULTS

We used CELLAVISTA® for live imaging of actin, which we stained with the fluorogenic labelling probe SiR-actin. For good images, we inhibited the efflux pumps by verapamil. SiR-actin properly stained the actin filaments of CHO-K1 cells and structures like stress fibers were visible (Fig. 2).

We also observed multiple cells with actin re-organization during mitosis (Fig. 3). During early phases of mitosis, when cells started to round up and DNA was condensed into chromosomes, stress fibers diminished and instead, we saw a bright circular actin signal at the cell periphery. Most likely, this signal resembles the actomyosin network at the cell cortex, which is required to stabilize the round cellular form during mitosis [4]. During cytokinesis, we observed a strong actin signal in the cleavage furrow, most likely due to the role of actin in the contractile ring (Fig. 3).

After imaging untreated cells to visualize stress fibers and contractile rings, we treated cells with cytochalasin D. Cytochalasin D inhibited actin polymerization and depolymerized actin as early as 30 min after treatment (Fig. 4). Stress fibers were diminished and the actin staining became more punctate and condensated. As Hoechst33342 can be toxic to cells during live cell imaging [15],

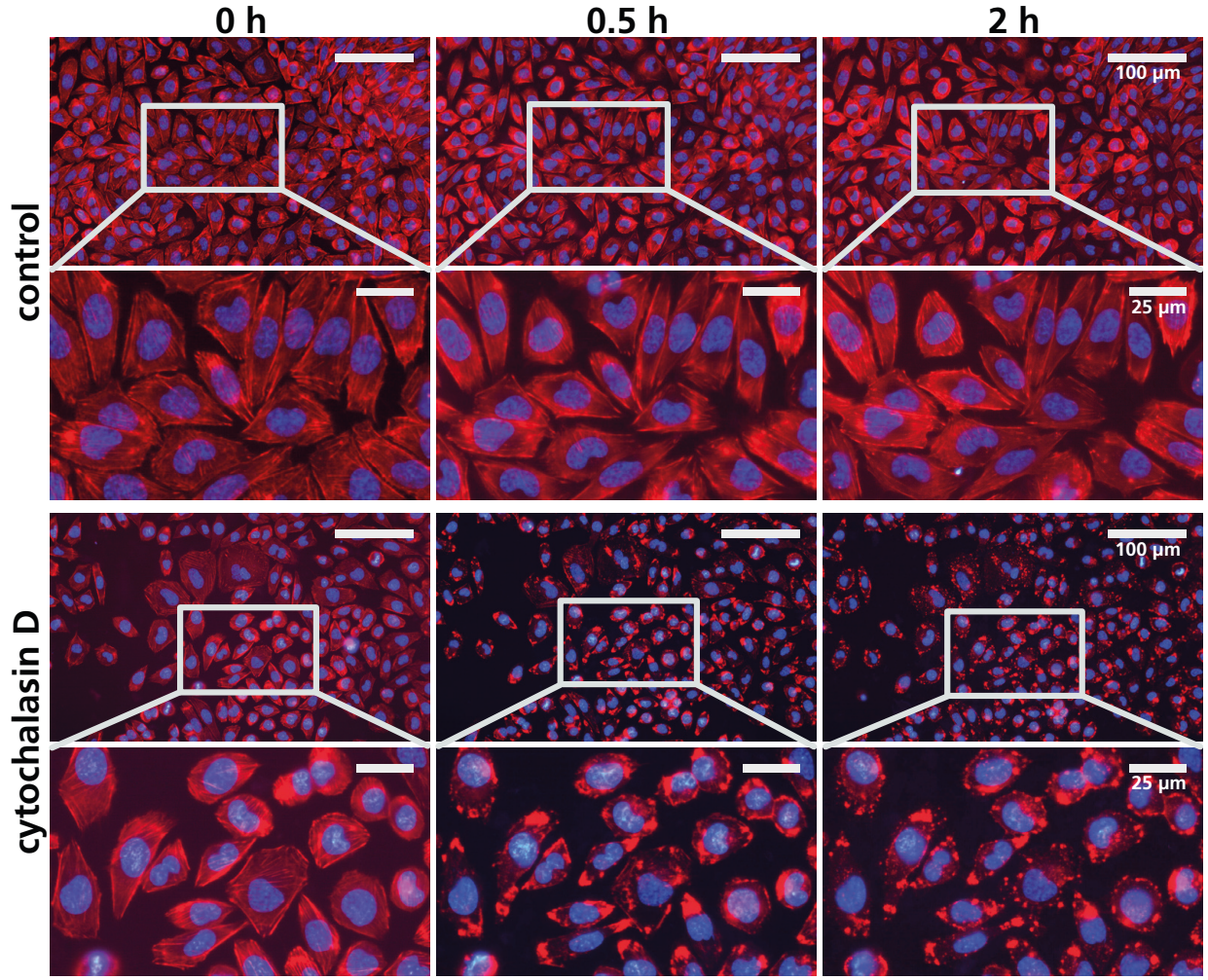

FIG. 4. SiR-ACTIN- AND HOECHST-STAINED CELLS DURING CYTOCHALASIN D TREATMENT

We stained CHO-K1 cells for one hour with SiR-actin plus verapamil and Hoechst. The cells were imaged using CELLAVISTA® before and during treatment with 0.5 µM cytochalasin D at the indicated time points. Compared with the control cells, the treated cells lost structures of polymerized actin (e.g. stress fibers) and the actin signal became more punctuate. More details are visible by zooming into the picture within YT®-software (40x objective, upper row scale bar: 100 µm, lower row scale bar: 25 µm).

we alternatively stained cells with SiR-actin and SPY505-DNA, which is an available DNA-dye for live imaging (Fig. 5). We observd similar results for both DNA dyes.
The intensity of the SiR-actin signal increased during the treatment with cytochalasin D. The proportion of F-actin decreased and the cells were losing their flat shape. These morphological changes could also be quantified using the *Real Cytoplasm (1F)* application of YT®-software (Fig. 6). The software detects the nuclei and the SiR-actin-stained cytoplasm. The nuclei of the processed cells are encircled by a green line (if no surrounding cytoplasm is detected) or orange (if a SiR-actin-stained cytoplasm is detected). The cell border as recognized by actin staining is marked by a purple line (single cell, only one detected nucleus) or a light blue line (cell cluster, more than one detected nucleus inside the marked area).
The analysis showed that cytochalasin D-treated cells had a higher median SiR-actin intensity than the control cells (28 versus 12.9, respectively, background corrected - BC) (Fig. 6). The standard deviation also shows a higher variety of the pixel values (intensities) for the marked areas after treatment (treated 16.8 versus control 7.31). These results correspond to the fact, that the loss of F-actin let to rounded cell forms with smaller cell areas but high condensed actin.

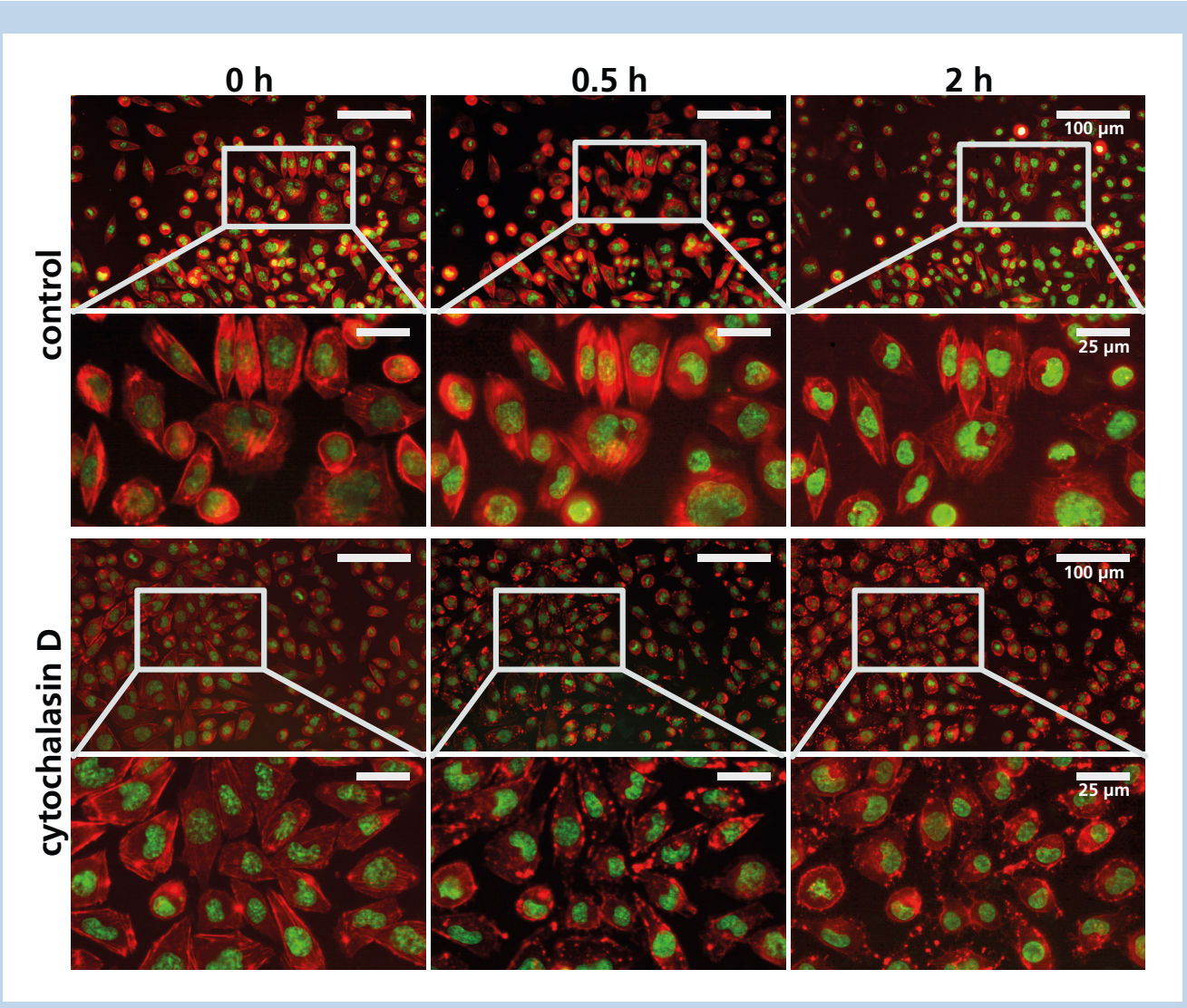

FIG. 5. SiR-ACTIN- AND SPY505-DNA-STAINED CELLS DURING CYTOCHALASIN D TREATMENT

We stained CHO-K1 cells for one hour with SiR-actin plus verapamil and SPY505-DNA. The cells were imaged using CELLAVISTA® before and during treatment with 0.5 µM cytochalasin D at the indicated time points. Compared with the control cells, the treated cells lost structures of polymerized actin (e.g. stress fibers) and the actin signal became more punctuate. More details are visible by zooming into the picture within YT®-software (40x objective, upper row scale bar: 100 µm, lower row scale bar: 25 µm).

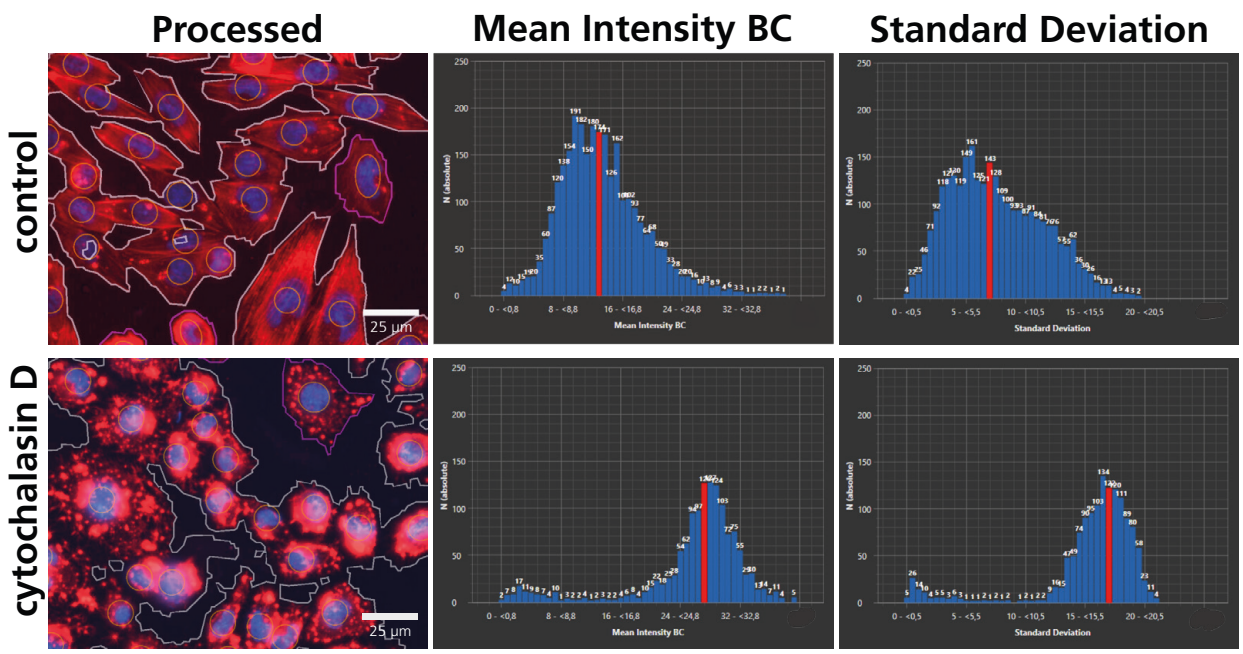

FIG. 6. SiR-ACTIN-STAINED CELLS DURING CYTOCHALASIN D TREATMENT

Analysis of imaged cells was performed using the *Real Cytoplasm (1F)* application of YT®-software. Here, the cells were imaged using NYONE® (left, 20x objective, scale bar: 25 µm) and afterwards processed using the *Real Cytoplasm (1F)* application. Blue Hoechst33342-stained nuclei are encircled in orange and the red SiR-actin-stained cytoplasm is surrounded by a purple (single cell) or light blue line (cell cluster). YT®-software determines the mean intensity (BC – background corrected) of the cytoplasm area and its standard deviation. Cytochalasin D-treated cells had a higher mean intensity and standard deviation compared with control cells.

CONCLUSION

SYNENTEC's cell imagers enable live cell imaging and analysis of actin dynamics over time. We could image the different structures of actin by using the fluorescently labelled SiR-actin probe. Cytochalasin D-induced changes in the actin cytoskeleton were clearly visible and were quantified using the *Real Cytoplasm (1F)* application of YT®-software. Thus, SYNENTEC's imagers in combination with fluorescent dyes are a powerful tool to analyze drug-induced changes in the cytoskeleton.

CELLAVISTA® 4

NYONE®

References

[1] K. K. McKayed and J. C. Simpson, "Actin in Action: Imaging Approaches to Study Cytoskeleton Structure and Function," p. 17, 2013.

[2] Y.-W. Heng and Koh, Cheng-Gee, "Actin cytoskeleton dynamics and the cell division cycle," Int. J. Biochem., p. 12, 2010.

[3] L. Blanchoin, R. Boujemaa-Paterski, C. Sykes, and J. Plastino, "Actin Dynamics, Architecture, and Mechanics in Cell Motility," Physiol. Rev., vol. 94, no. 1, pp. 235–263, Jan. 2014, doi: 10.1152/physrev.00018.2013.

[4] O. M. Lancaster and B. Baum, "Shaping up to divide: Coordinating actin and microtubule cytoskeletal remodelling during mitosis," p. 7, 2014.

[5] J. F. Casella, M. D. Flanagan, and S. Lin, "Cytochalasin D inhibits actin polymerization and induces depolymerization of actin filaments formed during platelet shape change," Nature, vol. 293, no. 5830, pp. 302–305, Sep. 1981, doi: 10.1038/293302a0.

[6] S. Nonaka, H. Naoki, and S. Ishii, "A multiphysical model of cell migration integrating reaction–diffusion, membrane and cytoskeleton," Neural Netw., vol. 24, no. 9, pp. 979–989, Nov. 2011, doi: 10.1016/j.neunet.2011.06.009.

[7] M. Melak, M. Plessner, and R. Grosse, "Actin visualization at a glance," J. Cell Sci., vol. 130, no. 3, pp. 525–530, Feb. 2017, doi: 10.1242/jcs.189068.

[8] T. Ikeno, T. Nagano, and K. Hanaoka, "Silicon-substituted Xanthene Dyes and Their Unique Photophysical Properties for Fluorescent Probes," Chem Asian J, p. 12, 2017.

[9] G. Lukinavičius et al., "A near-infrared fluorophore for live-cell super-resolution microscopy of cellular proteins," Nat. Chem., vol. 5, no. 2, pp. 132–139, Feb. 2013, doi: 10.1038/nchem.1546.

[10] G. Lukinavičius et al., "Fluorogenic probes for live-cell imaging of the cytoskeleton," Nat. Methods, vol. 11, no. 7, pp. 731–733, Jul. 2014, doi: 10.1038/nmeth.2972.

[11] L.-G. Milroy et al., "Selective Chemical Imaging of Static Actin in Live Cells," J. Am. Chem. Soc., vol. 134, no. 20, pp. 8480–8486, May 2012, doi: 10.1021/ja211708z.

[12] J. A. Cooper, "Effects of cytochalasin and phalloidin on actin.," J. Cell Biol., vol. 105, no. 4, pp. 1473–1478, Oct. 1987, doi: 10.1083/jcb.105.4.1473.

[13] M. Trendowski, "Using Cytochalasins to Improve Current Chemotherapeutic Approaches," Anticancer Agents Med. Chem., vol. 15, no. 3, pp. 327–335, Mar. 2015, doi: 10.2174/1871520614666141016164335.

[14] Spirochrome AG, "SPY505-DNA datasheet", https://spirochrome.com/documents/202003/datasheet_SPY505-DNA_202003.pdf (accessed Dec. 04, 2020).

[15] M. Purschke, N. Rubio, K. D. Held, and R. W. Redmond, "Phototoxicity of Hoechst 33342 in time-lapse fluorescence microscopy," Photochem. Photobiol. Sci. Off. J. Eur. Photochem. Assoc. Eur. Soc. Photobiol., vol. 9, no. 12, pp. 1634–1639, Dec. 2010, doi: 10.1039/c0pp00234h.

Acknowledgement

We thank Spirochrome for free samples of SiR-actin and SPY505-DNA (see https://spirochrome.com/product/sir-actin-50-nmol/ or https://spirochrome.com/product/spy505-dna/ for details).
This work was part of a cooperation project with the Institute for Experimental Tumor Research (IET). We thank the IET for outstanding support, fruitful discussions and a great working atmosphere during this cooperation.

Institut für Experimentelle Tumorforschung

published 01/2021

SYNENTEC GmbH
Otto-Hahn-Str. 9A
25337 Elmshorn/Germany
Phone. +49 (0) 4121 46311-0
Email. appsupport@synentec.com

www.synentec.com